

## Analysis of Noise Reduction Methods for Blasting Vibration Signals in Tunnels Separated by Small Clear Distances

Chenyang Dong<sup>1</sup>, Hui Xiang<sup>1</sup>, Jian Cui<sup>1</sup>, Wei Hu<sup>2</sup> and Yayu Miao<sup>2,\*</sup>

<sup>1</sup>China State Construction Railway Investment & Engineering Group Co., Ltd, Beijing 100053, China

<sup>2</sup>Hunan Province Key Laboratory of Geotechnical Engineering Stability Control and Health Monitoring, Hunan University of Science and Technology, Xiangtan 411201, China

Received 13 May 2024; Accepted 4 July 2024

### Abstract

The construction environment of tunnels is complex due to their unique spatial constraints, the diversity of rock properties, and the variability of construction machinery, which jointly lead to a substantial amount of noise contained in the measured tunnel blast vibration signals, resulting in distortion of the signal characteristics. This study proposed a method to analyze the noise reduction effect through the noise reduction objective function index after decomposition and reorganization of the original signal to accurately analyze the characteristics of tunnel blasting vibration signals. The original signal was decomposed into several intrinsic modal functions (IMFs) with varying frequencies and amplitudes by utilizing empirical modal decomposition (EMD) and variational modal decomposition (VMD) for noise reduction. These IMFs were then restructured, and noise reduction metrics were employed to analyze the noise reduction effect. Results demonstrate that both algorithms can effectively reduce the noise of the original signal at different sampling frequencies. The correlation coefficients of the EMD and VMD methods remain above 0.8526 and 0.9940, respectively. With the increase in sampling frequency, the VMD method exhibits greater stability in noise reduction processing compared to the EMD method, especially at high sampling frequencies. Thus, the noise reduction effect of the VMD method is substantial. The proposed method provides a good reference for similar engineering blasting vibration signal noise reduction processing.

*Keywords:* Blasting vibration, Noise reduction methods, Empirical modal decomposition Variational modal decomposition

### 1. Introduction

Blasting technology is widely employed during tunnel excavation due to its high efficiency. However, blasting operations inevitably have an adverse impact on the surrounding environment and buildings [1, 2], therefore, accurate monitoring and analysis of blasting vibration signals is of considerable importance to ensure construction safety and reduce environmental impact.

A major challenge in the monitoring and analysis of blast vibration signals is that the signals often contain large amounts of noise. The occurrence of these noises can be attributed to a multifaceted range of influencing factors, such as instrument errors, reflections transmitted by the medium, and disturbances in the construction environment, increasing the difficulty in accurately extracting and analyzing the signals. Noise reduction processing is a necessary step to accurately analyze the characteristics of vibration signals [3, 4]. Blast vibration signals are nonstationary, which indicates that the statistical characteristics of the signal (e.g., mean, variance) vary with time. This nonsmoothness limits the effectiveness of traditional signal processing methods (e.g., Fourier transform) in noise reduction processing.

Blast vibration signals are generally processed using empirical modal decomposition (EMD) [5, 6]. The EMD method encounters the challenge of modal aliasing. This issue manifests itself in the presence of signals exhibiting diverse scale distributions within the same Intrinsic Mode

Function (IMF) component, or signals with similar scales but occurring in distinct IMF components. The presence of modal aliasing not only leads to a false time–frequency distribution but also renders the IMFs physically meaningless. Another commonly used signal processing method, variational modal decomposition (VMD), suppresses modal aliasing by introducing a regularization term that constrains the bandwidth or frequency range of the modal functions and reduces the spectral overlap between different modal functions. Lei et al. [7] adopted the algorithm of VMD and improved the accuracy and efficiency of signal separation by introducing an optimization algorithm to construct the fitness function. This algorithm utilizes the energy difference parameter and the sample entropy to achieve the optimal adjustment of the modal number and the penalty factor. The modal aliasing problem of EMD limits its application in the analysis of complex signals. The VMD algorithm improves the shortcomings of EMD to a certain extent but fails to completely separate the signal from the noise. Therefore, comparing and analyzing the noise reduction effects of the two algorithms for blasting vibration signals is necessary to realize the optimal effect of noise reduction processing.

Based on the above analysis, this study first decomposes the blast vibration signals using EMD and VMD. These signals are then compared and analyzed by reorganizing the IMFs and the noise reduction indexes to obtain the optimal noise reduction signals. The proposed method is applied to the noise reduction processing of the blast vibration signals of the measured tunnels.

\*E-mail address: myy6308@163.com

ISSN: 1791-2377 © 2024 School of Science, DUTH. All rights reserved.

doi:10.25103/jestr.173.07

## 2. State of the art

Scholars have conducted numerous studies on improving EMD and VMD to achieve excellent noise reduction.

In the process of in-depth investigation of noise reduction techniques based on EMD and independent component analysis, Jia et al. [8] found that noise can be effectively reduced but transient non-smooth features are retained. However, they did not quantitatively analyze the noise reduction effect of the EMD and VMD methods. Li et al. [9] compared and analyzed the wavelet and EMD filtering methods and found that each of the two methods demonstrated unique advantages in noise reduction. However, the specific process of utilizing IMFs was not comprehensively explored and elaborated. Zhao et al. [10] proposed an improved EMD noise reduction method combining EMD thresholding noise reduction and Savitzky–Golay filtering noise reduction, which was optimized by targeting high-frequency and low-frequency modal functions (IMFs). Simulation experiments showed that this improved method outperforms either the EMD thresholding method or the Savitzky–Golay filtering method alone in terms of noise reduction performance. However, in-depth comparative studies of how EMD and VMD acquire and utilize IMFs during signal processing are lacking. Xu [11] proposed EEMD as an improved method for the modal aliasing problem of EMD when the signal is interrupted. Despite the unique advantages of EEMD and VMD in noise reduction and modal decomposition, these methods are not further optimized to fit the signal characteristics in specific application scenarios. The VMD smooth noise reduction model proposed by Peng et al. [12] showed noise reduction capability in tunnel blasting signals. Regardless of the generally successful performance of the VMD model, the effectiveness of its application in the special environment of small-clearance separated tunnels should be further verified. Deng et al. [13] used the particle swarm algorithm and wavelet threshold denoising combined with VMD to process microseismic signals. However, they did not compare the variations, advantages, and disadvantages of the different methods for IMF processing. The VMD–SVD–Robust ICA method proposed by Li et al. [14] effectively separated the mixed signals but lacked application in small-clearance separated tunnels. Karan et al. [15] combined VMD and BiDLSTM deep learning algorithms to improve prediction accuracy but did not compare the differences in IMF processing between the methods. Amitha et al. [16] used VMD to detect power signal pulse transients but failed to improve the VMD technique to obtain effective noise reduction. Mohamed et al. [17] improved the accuracy of modal identification by integrating independent component analysis (ICA) with MEMD for the modal aliasing problem in EMD, but the noise reduction effect for specific environments was understudied. Mohsen et al. [18] explored the application of VMD in detecting localized structural damage. The time course of acceleration in a bridge span was decomposed into IMFs by VMD. They found that the instantaneous frequency and instantaneous amplitude of the first-order IMF exhibited irregularities at the damage location, which demonstrated the superiority of VMD in damage detection compared to the EMD method. However, this study was limited in its noise reduction analysis. Giaouris et al. [19] investigated the potential of wavelet analysis for applications in electric drive systems, especially

in addressing the problem of corrupted current signals due to noise caused by defective sensors. They compared wavelet analysis with classical methods and demonstrated the advantages of wavelet analysis in handling useful information with time-varying high-frequency characteristics. However, when the signal contains nonlinear and non-smooth characteristics, wavelet analysis may only partially extract useful information compared to EMD and VMD. Mpoyi et al. [20] utilized EMD and FDM to monitor tool wear, but validation was limited to a single method and did not compare multiple methods. The hybrid model based on EMD and SVR by Redekar et al. [21] performed well in the prediction of PV array pollution. However, further improvement in noise reduction is necessary to improve the accuracy of the prediction model. Shamaee et al. [22] proposed an adaptive denoising method based on deep learning and the EMD method, using dominant noise to enhance the EMD. This method identifies the dominant noise through pattern decomposition and a two-step LSTM classifier. Subsequently, the detected features were used for noise-assisted pattern decomposition, and the most relevant components of the dominant noise were adaptively removed. The method effectively classified and suppressed white and colored noise. However, the robustness and stability of this noise reduction method must still be further verified.

The above studies were mainly based on the improvement of two signal processing methods, namely EMD and VMD, to obtain satisfactory noise reduction effects. However, studies that quantitatively analyze the noise reduction effects of the two methods in small-clearance separated tunnels are still relatively few. In particular, comparative studies of how the two methods obtain and use IMFs when processing signals lack in-depth discussions. In this study, the original signal is decomposed into multiple IMFs with different frequencies and amplitudes by using two noise reduction methods, namely EMD and VMD. These IMFs are then reorganized to obtain the optimal noise reduction signal, and the noise reduction metrics are used to analyze the noise reduction effect.

The remainder of this study is organized as follows. Section 3 describes the basic principles of EMD and VMD, along with the evaluation indexes employed to evaluate the noise reduction effect. In Section 4, the noise reduction of blast vibration signals is conducted using EMD and VMD for this engineering example, and the noise reduction processing effects of blast vibration signals under different methods are obtained. The final section summarizes the study and presents relevant conclusions.

## 3. Methodology

### 3.1 EMD Rationale

EMD is a novel method for handling nonstationary signals that can decompose the signal based on its inherent time-scale characteristics without relying on any pre-set basis functions. The core of this method lies in empirical mode decomposition (EMD), which facilitates the decomposition of complex signals into a finite number of intrinsic modal functions (IMFs). Each decomposed component of an IMF contains localized characteristic signals of the original signal at varying time scales [23, 24].

Identifying the extreme values and extreme points of the signal is essential to identifying the local characteristics and fluctuation range of a signal. The upper and lower envelopes of the signal can be constructed by utilizing curve

interpolation to fit these extreme points. These envelopes can then serve as an approximation of the fluctuation range of the signal.

The peak and trough points of the original signal  $f(t)$  are then connected to these extreme points through curve interpolation to obtain the upper envelopes  $f_{\max}(t)$  and lower envelopes  $f_{\min}(t)$  of the signal.

The upper and lower envelopes are averaged to isolate the long-term trend or overall variation of the signal from the original signal and accurately extract the IMFs in subsequent steps.

$$s(t) = \frac{f_{\max}(t) + f_{\min}(t)}{2} \quad (1)$$

In signal processing, a residual signal can be obtained by performing a subtraction operation between the original signal and the mean envelope calculated by interpolating between the extreme points. For smooth signals, this residual signal often directly reflects the characteristics of the original signal in a specific frequency range and is extracted as the first IMF of the original signal. However, the situation differs when dealing with signals that exhibit irregularities. A signal with a non-monotonic waveform, which is characterized by inflection points at specific locations, contains important features of the original signal. If these inflection points are not precisely captured during the processing stage, then the resulting first-order IMF may fail to accurately represent the characteristics of the original signal at this frequency scale. Specifically, this condition may not adhere to the two fundamental criteria of an IMF: (1) the number of extreme points and zero crossings must differ by at most one, and (2) the local mean value should be zero. Therefore, further optimizing and extracting the IMF through a screening process is necessary to ensure the accuracy and validity of the IMF. This process is repeated on the remaining signals  $v(t)$  until the stopping criterion (SD, generally taking a value between 0.2 and 0.3) falls below the threshold value, thus obtaining the final first-order modal component  $\omega(t)$  (i.e., the first IMF). The SD is calculated as follows:

$$SD = \sum_{i=0}^T \left[ \frac{|v_{k-1}(t) - v_k(t)|^2}{v_{k-1}^2(t)} \right] \quad (2)$$

The first-order residual quantity  $\rho(t)$  is obtained by subtracting signal  $\omega(t)$  from signal  $f(t)$ . Instead of the original signal  $f(t)$ ,  $\rho(t)$  can be used as the input for the subsequent processing steps to obtain the  $n$ th-order modal function  $\omega_n(t)$  and the final standardized residual quantity  $\rho_n(t)$  after repeating the process for  $n$  times. The mathematical expression for the decomposition of the original signal  $f(t)$  using empirical mode decomposition (EMD) is as follows:

$$f(t) = \sum_1^n \omega_n(t) + \rho_n(t). \quad (3)$$

### 3.2 VMD Rationale

VMD is an adaptive, fully non-recursive method for modal discretization and signal processing. The algorithm can

determine the number of modal decompositions based on the actual situation, thus exhibiting its adaptivity. Furthermore, the subsequent iteration and solving process enables the algorithm to adaptively match the optimal center frequency and finite bandwidth of each modality. Additionally, VMD efficiently separates IMFs, partitions signals into frequency bands, extracts key decomposition components, and achieves the optimal variational solution [25, 26].

The variational problem is first constructed by assuming that the original signal  $f$  is decomposed into  $K$  components, where each component is an IMF with a finite bandwidth and a center frequency. The objective is to minimize the sum of the estimated bandwidths of the IMFs while satisfying the constraint that the sum of all the modes is equal to the original signal. The corresponding constrained variational expression is then derived as follows:

$$\min_{\{\mu_k\}, \{\omega_k\}} \left\{ \sum_k \left\| \partial_t [\delta(t) + j / \pi(t) * \mu_k(t)] e^{-j\omega_k t} \right\|_2^2 \right\} \quad (4)$$

$$s.t. \sum_{k=1}^K \mu_k = f$$

where  $\{\mu_k\}, \{\omega_k\}$  represent the  $(k)$ -th IMF component and center frequency, respectively, after decomposition.

The Lagrange multiplier  $\lambda$  is introduced to transform the constrained variational problem into an unconstrained variational problem and solve the above equation, and the augmented Lagrangian function is obtained as:

$$L(\{\mu_k\}, \{\omega_k\}, \lambda) = \alpha \sum_k \left\| \partial_t [\delta(t) + j / \pi(t) * \mu_k(t)] e^{-j\omega_k t} \right\|_2^2 \quad (5)$$

$$+ \left\| f(t) - \sum_k \mu_k(t) \right\|_2^2 + \left\langle \lambda(t), f(t) - \sum_k \mu_k(t) \right\rangle$$

where  $\alpha$  is a quadratic penalty factor that serves to reduce the interference of Gaussian noise. The alternating direction method of multipliers (ADMM), combined with Parseval's theorem (or Plancherel's theorem), optimizes modal components as well as center frequencies. Additionally, this algorithm is employed to search for the saddle point of the augmented Lagrangian function. The expressions of  $\mu_k$ ,  $\omega_k$  and  $\lambda$  after the ADMM iteration are as follows:

$$\hat{\mu}_k^{n+1}(\omega) \leftarrow \frac{\hat{f}(\omega) - \sum_{i \neq k} \hat{\mu}_i(\omega) + \hat{\lambda}(\omega) / 2}{1 + 2\alpha(\omega - \omega_k)^2}$$

$$\hat{\lambda}^{n+1}(\omega) \leftarrow \hat{\lambda}^n + \gamma(f(\omega) - \sum_k \hat{\mu}_k^{n+1}(\omega)) \quad (6)$$

$$\omega_k^{n+1} \leftarrow \frac{\int_0^\infty \omega \left| \hat{\mu}_k^{n+1}(\omega) \right|^2 d\omega}{\int_0^\infty \left| \hat{\mu}_k^{n+1}(\omega) \right|^2 d\omega}$$

The main iterative solution process of the VMD is as follows:

S1: Initialization of  $\hat{\mu}_k^1, \hat{\omega}_k^1, \lambda^1$  and maximum number of iterations  $N, n \leftarrow 0$ ;

S2: Using Equation (6) to update  $\hat{\mu}_k, \hat{\omega}_k, \hat{\lambda}$ ;

S3: Precision convergence criterion  $\varepsilon > 0$ ; if it does not meet conditions  $\sum_k \left\| \hat{\mu}_k^{n+1} - \hat{\mu}_k^n \right\|_2 / \left\| \hat{\mu}_k^n \right\|_2 < \varepsilon$  and  $n < N$ , then return to the second step; otherwise, complete the iteration and output the final result  $\hat{\mu}_k, \hat{\omega}_k$ .

### 3.3 Noise Reduction Indexes

Linear correlation coefficient is a quantity that examines the degree of linear correlation between variables. This coefficient is usually denoted by  $r$ .

$$r(X,Y) = \frac{Cov(X,Y)}{\sqrt{Var[X]Var[Y]}} \quad (7)$$

where  $Cov(X,Y)$  is the covariance of  $X,Y$ , and  $Var[X], Var[Y]$  is the variance of  $X,Y$ .

The mean squared error (MSE) measures the magnitude of dissimilarity between the noise-reduced and original functions. In the context of geotechnical engineering, MSE can be used as an indicator of the accuracy of noise reduction algorithms applied to signals.

$$MSE = \sqrt{\frac{\sum_n (y_i - y'_i)^2}{n}} \quad (8)$$

where  $y_i$  and  $y'_i$  denote the signal after noise reduction and the original signal, respectively.

The noise reduction objective function  $f$  [26, 27] is defined as a weighted combination of factors. In this function,  $\alpha$  represents the algorithm performance factor with a value of 0.2, and  $\beta$  represents the correlation coefficient factor with a value of 0.8.

$$\max\{f\} = \max\{\alpha MSE_f^{-1} + \beta |r|\} \quad (9)$$

### 3.4 EMD Signal

The sampling frequency of the measured signal is 10,000 Hz. A time span of 0 to 1.4 s is selected for noise reduction of the signal, as depicted in Fig. 1. A total of 14,334 sampling points were collected during this period.

The original signal is decomposed using the EMD algorithm, and the resulting time domain diagram of the vibration signal decomposition is presented in Fig. 2. As shown in the figure, the EMD algorithm effectively separates the original signal into multiple IMF components, each carrying distinct signal characteristics.

However, the endpoint effect is one of the issues encountered with EMD. The EMD decomposes the signal into IMFs sequentially through a series of sifting processes, where the local average of the signal is calculated based on its upper and lower envelopes. The envelopes of a signal are delineated by its local maxima and minima, employing spline interpolation. Notably, both extremities of the signal cannot concurrently attain extreme maximum and minimum

values. Thus, the upper and lower envelopes inevitably diverge at the endpoints of the data sequence. Consequently, this divergence directly impacts the quality of the EMD [28].

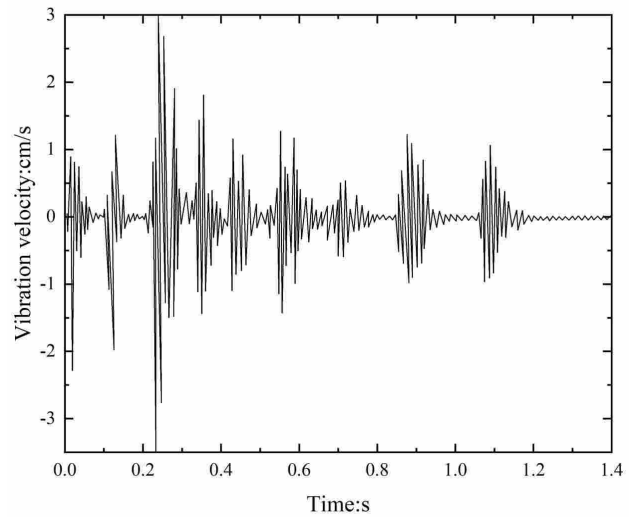


Fig. 1. Bursting signal

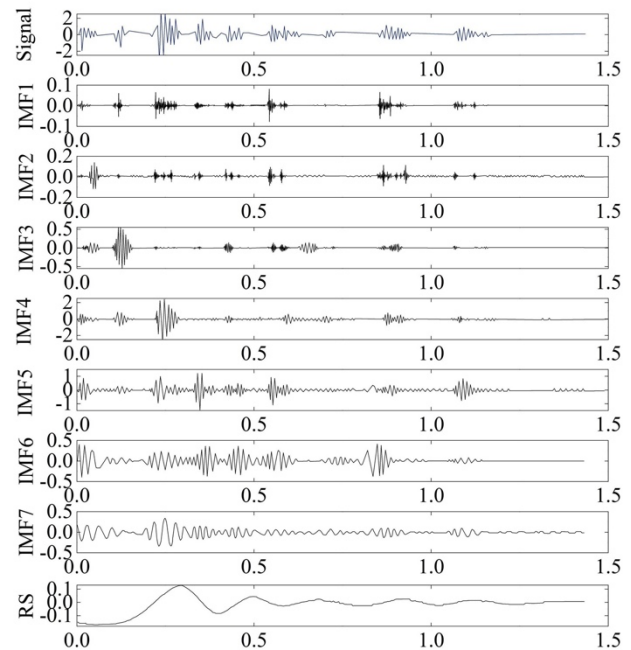


Fig. 2. EMD time-domain diagram

### 3.5 VMD Decomposition Signal

The parameters should be set before decomposing the signal using the VMD algorithm. The fidelity  $\tau$  is set to 0, and the penalty factor  $\alpha$  is set to the default value of 2000. The determination of the number of modes  $K$  is obtained based on the center frequency method, as shown in Table 1. When  $K = 8$ , the highest center frequency increases abruptly, indicating over-decomposition; therefore, the value of  $K$  is set to 7. At this point, the change in center frequency is shown in Fig. 3. The decomposition of the time-domain graph is depicted in Fig. 4, where the last component represents the low-frequency noise part. The VMD algorithm is highly effective at decomposing signals, and it can extract the low-frequency noise component.

As observed from the frequency domain plot in Fig. 5, each IMF component possesses a distinct center frequency. Each IMF exhibits a considerably narrow frequency band, and no modal aliasing phenomenon is observed.

Fig. 6 presents a three-dimensional comparison of each IMF component with the original signal. Analysis results reveal that the IMF components can be grouped into three parts: IMF1 to IMF4 correspond to the initial stage of the blasting process; IMF5 represents the second part, which demonstrates the most notable impact; and IMF6 to IMF7 correspond to the third part, where the energy is reduced, and the effects of blasting vibration gradually diminish.

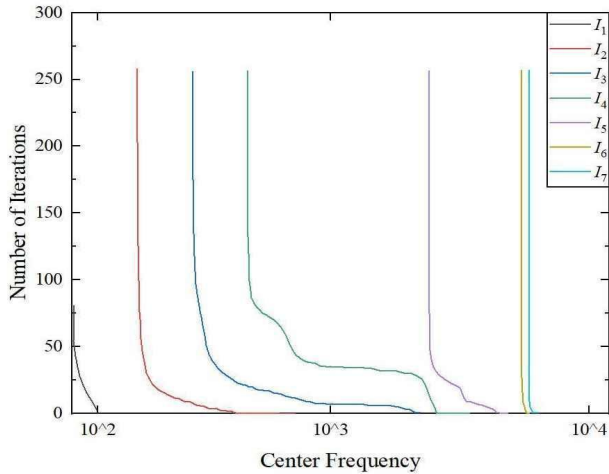


Fig. 3. Plot of change in center frequency

Table 1. Center frequencies of components at different values of  $K$

$K$	$I_1$	$I_2$	$I_3$	$I_4$	$I_5$	$I_6$	$I_7$	$I_8$
2	89.252	160.515						
3	88.336	151.261	355.368					
4	88.201	149.645	312.212	1452.371				
5	88.141	148.021	266.426	508.023	1413.877			
6	88.141	147.172	247.642	413.644	761.670	1459.689		
7	88.128	143.663	181.105	280.601	439.239	765.566	1462.222	
8	88.097	142.750	176.979	276.528	436.841	763.171	1447.586	3319.976

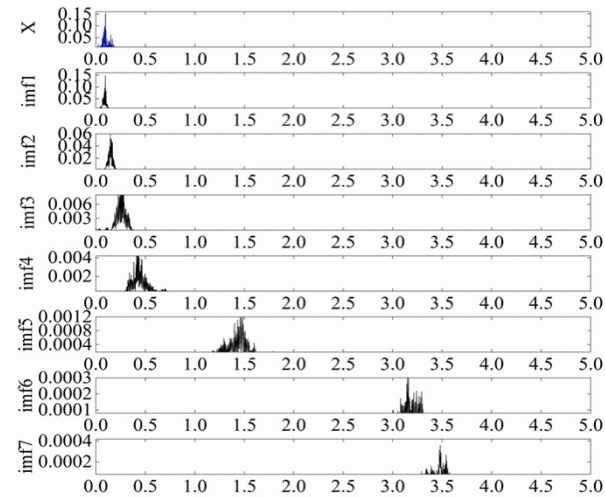


Fig. 5. Frequency-domain graph

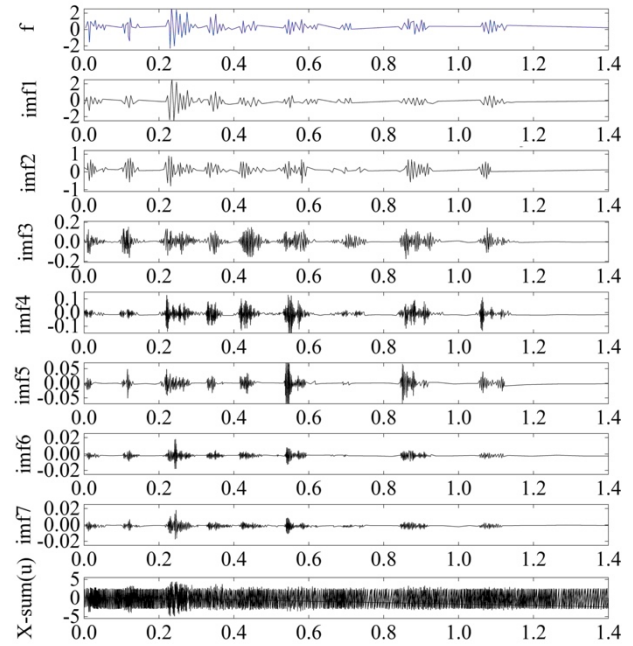


Fig. 4. VMD time-domain diagram

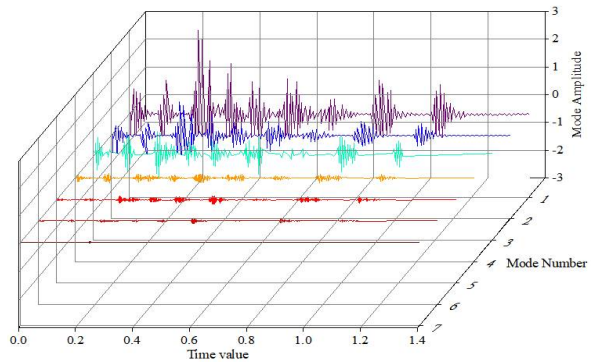


Fig. 6. VMD 3D component comparison

## 4. Result Analysis and Discussion

### 4.1 Project Cases

The Xiangshuling Tunnel is located in Nanchuan District, Chongqing. For this small-clearance separated rock tunnel, the tunnel traverses through various types of rocks, ranging from hard to soft, mainly comprising V- and IV-level surrounding rock. Table 2 shows the length of the surrounding rock sections and their proportion of the total tunnel length.

Table 2. Distribution of surrounding rocks at all levels of the tunnel

Rock mass classification	Left line		Right line	
	Lengths	Percentage of	Lengths	Percentage of

		total length		total length
V	734 m	18.26%	660 m	16.45%
IV	3285 m	81.74%	3351 m	83.55%

Grade V surrounding rock is primarily distributed at the entrance and exit of the cave. The stratum lithology mainly comprises siltstone, mudstone, and shale, which are classified as soft rocks. Tectonic fractures are highly developed, resulting in poor interlayer bonding, and the surrounding rock exhibits poor self-stabilizing capability, increasing its collapse tendency. Therefore, the construction adopts the three-bench and seven-segment excavation method, which involves arc-shaped pilot excavation to retain the core soil as the basic mode. This method is divided into upper, middle, and lower steps with seven excavation surfaces. Each excavation and support phase is staggered longitudinally along the tunnel, proceeding parallel to the advancement of the tunnel construction.

Several residences are found near the tunnel. The L-20 vibrometer was used on-site for testing to evaluate the impact on the surrounding environment during tunnel blasting and excavation. A typical blasting vibration signal was selected as the study object. The monitoring points are depicted in Fig. 7, while the blasting signal and amplitude spectrum are presented in Fig. 8 and Fig. 9, respectively.

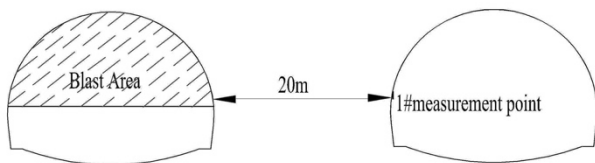


Fig. 7. Location of monitoring points

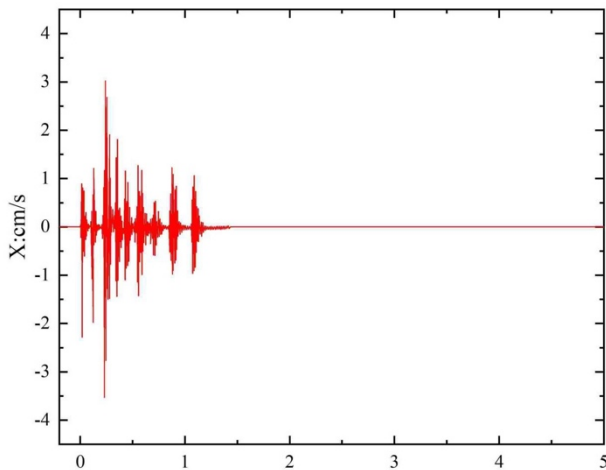


Fig. 8. Measured blast signal

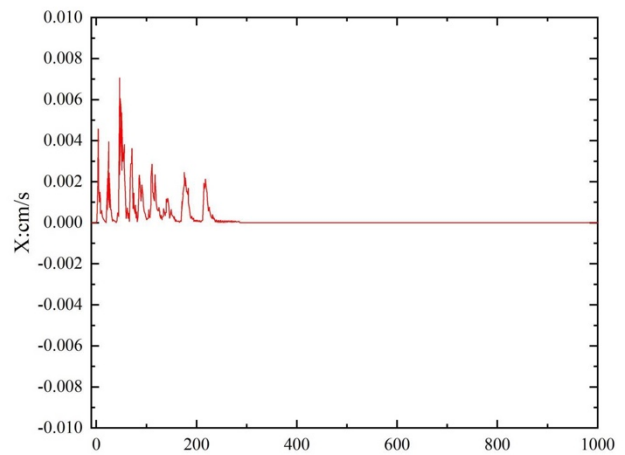


Fig. 9. Amplitude spectrum

#### 4.2 Noise Reduction of Blast Vibration Signals

The individual components decomposed by the two algorithms are reorganized and subsequently compared to the original signal to achieve noise reduction. The superposition of IMF1 through IMF7 is denoted as Fs17, the superposition of IMF2 through IMF7 is denoted as Fs27, and so forth up to Fs67, as illustrated in Fig. 10 and Fig. 11.

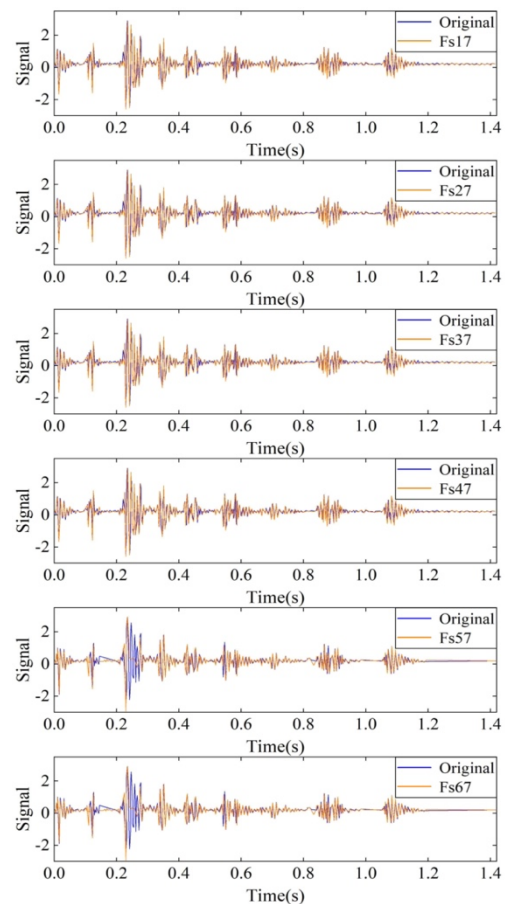


Fig. 10. Comparison of EMD reconstructed and original signals

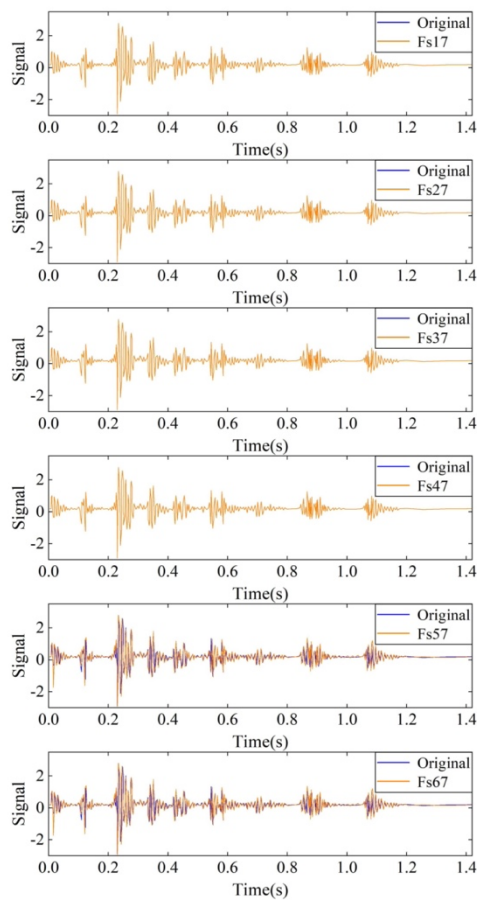


Fig. 11. Comparison of VMD reconstructed and original signals

From Fig.10 and Fig. 11, it can be seen that compared to the VMD method, the EMD recombined signal notably diverges from the original signal after Fs47 and begins to exhibit distortion, indicating that the VMD recombined signal has a superior correlation with the original signal compared to EMD. The noise reduction metrics in Table 3 reveal that VMD outperforms the EMD algorithm for each recombined signal. Despite the adaptive binary filtering characteristics of the EMD method, for complex signals, noise and impulse interference can affect the envelope calculation. This phenomenon subsequently impacts modal decomposition, leading to aliasing and rendering the IMF component devoid of its physical significance. By contrast, VMD is a set of adaptive Wiener filters with strong noise robustness. The modal and center frequencies are continuously adjusted and updated using this method to achieve a superior signal decomposition effect [28, 29]. This finding conclusively demonstrates that the VMD algorithm is more advantageous than the EMD algorithm in noise reduction processing.

Table 3. Noise reduction indicator

Project		Fs17	Fs27	Fs37	Fs47	Fs57	Fs67
EMD	M	0.9935	0.9935	0.9932	0.9891	0.9011	0.8526
	r	0.9828	0.9826	0.9818	0.9704	0.6478	0.2889
	f	0.9850	0.9848	0.9841	0.9742	0.6985	0.4016
VMD	M	1.000	0.9999	0.9997	0.9992	0.9975	0.9940
	r	1.000	0.9998	0.9993	0.9980	0.9934	0.9844
	f	1.000	0.9998	0.9994	0.9983	0.9942	0.9863

### 5. Conclusions

This study adopted two signal processing methods, namely EMD and VMD, to decompose and reorganize the IMFs and accurately analyze the characteristics of tunnel blasting vibration signals. The optimal noise reduction signals were obtained, and the noise reduction effects of these two methods on the blasting vibration signals of the engineering examples of the small-clearance separating tunnels were analyzed. The following conclusions could be drawn:

(1) Both signal processing methods can implement effective noise reduction processing on the original signal at various sampling frequencies. Specifically, the algorithmic similarity coefficients of the EMD and VMD methods are stable above 0.8526 and 0.9940, respectively, indicating a certain similarity and stability in noise reduction processing. The VMD method is superior to the EMD method in terms of decomposing and extracting IMFs; this method can also effectively reject low-frequency noise.

(2) The VMD method excels over the EMD method in terms of noise reduction, boasting a substantially larger linear correlation coefficient. Moreover, the linear correlation coefficient of the VMD method remains relatively stable with an increase in sampling frequency, exhibiting robust performance. Conversely, the linear correlation coefficient of the EMD method notably decreases

as the sampling frequency rises, indicating a decline in its noise reduction capabilities at high frequencies. As the sampling frequency increases, the VMD method demonstrates greater stability in noise reduction processing compared to the EMD method, particularly at high sampling frequencies.

In this study, the EMD and VMD decomposition of blasting vibration signals from the measured tunnels, along with a comparison of the two algorithms in terms of noise suppression and signal processing, provides a valuable reference for noise reduction processing of blasting vibration signals in similar projects. The current study primarily focuses on the noise reduction effect of blasting vibration signals over a single or short-term period; however, tunnel blasting is a long-term and continuous process. Therefore, future studies should test the algorithms for long-term stability to evaluate their performance in the continuous blasting process and explore potential improvement strategies.

### Acknowledgements

This work was supported by the National Natural Science Foundation of China (Grant Nos. 52378396).

This is an Open Access article distributed under the terms of the Creative Commons Attribution License.



## References

- [1] Q. Chen, H. T. Wang, G. Z. Hu, X. H. Li, K. X. Li, and C. Pang, "Monitoring and control technology of blasting vibration induced by tunnel excavation," *Rock. Soil. Mech.*, vol. 26, no. 6, pp. 964-967, Jan. 2005.
- [2] Y. P. Li, C. Z. Ai, C. L. Han, and M. Huo, "Numerical simulation study on dynamic effect of blasting excavation for small-spacing tunnels," *Explo. Shock.*, vol. 27, no. 1, pp. 75-81, Jan. 2007.
- [3] Y. J. Shen, S. P. Yang, and G. M. Zhang, "An adaptive signal denoising method based on fractional fourier transform," *J. Vib. Eng.*, vol. 22, no. 3, pp. 292-297, Jan. 2009.
- [4] X. Qin, J. C. Cai, S. Y. Liu, and A. F. Bian, "Study on the denoising method of microseismic signals based on empirical modal decomposition combined with mutual information entropy and synchronous compression transformation," *Geophys. Prospect. Petrol.*, vol. 56, no. 5, pp. 658-666, Sep. 2017.
- [5] N. E. Huang *et al.*, "The empirical mode decomposition and the Hilbert spectrum for nonlinear and non-stationary time series analysis," *Proc. Roy. Soc. London. Ser. A.*, vol. 454, no. 1971, pp. 903-995, Jan. 1971.
- [6] H. T. Liu, Z. W. Ni, and J. Y. Li, "Empirical mode decomposition method and its implementation," *Comput. Eng. Appl.*, vol. 42, no. 32, pp. 44-47, Jan. 2006.
- [7] Y. Lei, L. Liu, W. L. Bai, H. X. Feng, and Z. Y. Wang, "Analysis of high-speed railway seismic signals based on adaptive VMD algorithm," *Appl. Geophys.*, vol. 21, no. 2, pp. 358-371, Jun. 2024.
- [8] R. S. Jia, T. B. Zhao, H. M. Sun, and X. H. Yan, "Denoising method of microseismic signals based on empirical mode decomposition and independent component analysis," *Chinese. J. Geophys.-CH.*, vol. 58, no. 3, pp. 1013-1023, Jan. 2015.
- [9] X. B. Li, Y. P. Zhang, Y. J. Zuo, W. H. Wang, and Z. L. Zhou, "EMD filtering and denoising of rock blasting vibration signals," *J. Cent. South. Univ. Sci. T.*, vol. 37, no. 1, pp. 150-154, Jan. 2006.
- [10] Z. H. Zhao, S. P. Yang, and Y. J. Shen, "An improved EMD noise reduction method," *J. Vib. Shock.*, vol. 28, no. 12, pp. 35-37, Jan. 2009.
- [11] J. Xu, S. X. Huang, and F. H. Ma, "Analysis of dynamic characteristics of large bridges based on improved HHT theory," *Geomat. Inf. Sci. Wuhan. Univ.*, vol. 35, no. 7, pp. 801-805, Jan. 2010.
- [12] Y. X. Peng, G. J. Liu, Y. Su, Y. S. Liu, and C. Zhang, "A smooth denoising model for tunnel blasting vibration signals based on variational mode decomposition algorithm," *J. Vib. Shock.*, vol. 40, no. 24, pp. 173-179, Dec. 2021.
- [13] H. W. Deng and Y. P. Shen, "Denoising method of microseismic signals based on variational mode decomposition and particle swarm optimization algorithm," *Mining. Metall. Eng.*, vol. 41, no. 1, pp. 7-10, Feb. 2021.
- [14] S. C. Li, X. Wang, W. D. Guo, Z. Y. Tian, and S. S. Shi, "Research on advance geological detection technology of tunnel seismic while drilling in mechanized construction of drilling and blasting method," *Tunn. Constr.*, vol. 44, no. 4, pp. 617-632, Apr. 2024.
- [15] K. Sareen, B. K. Panigrahi, T. Shikhola, and A. Chawla, "A robust de-noising autoencoder imputation and VMD algorithm-based deep learning technique for short-term wind speed prediction ensuring cyber resilience," *Energy.*, vol. 283, Nov. 2023, Art. no. 129080.
- [16] A. Viswanath, K. J. Jose, N. Krishnan, S. S. Kumar, and K. P. Soman, "Spike detection of disturbed power signal using VMD," *Procedia Comput. Sci.*, vol. 46, pp. 1087-1094, 2015.
- [17] M. Barbosh, A. Sadhu, and M. Vogrig, "Multisensor-based hybrid empirical mode decomposition method towards system identification of structures," *Struct. Control. Hlth.*, vol. 25, no. 5, p. 21, Jan. 2018.
- [18] M. Mousavi, D. Holloway, J. C. Olivier, and A. H. Gandomi, "Beam damage detection using synchronisation of peaks in instantaneous frequency and amplitude of vibration data," *Measurement.*, vol. 168, Jan. 2021, Art. no. 128297.
- [19] D. Giaouris and J. W. Finch, "Denoising using wavelets on electric drive applications," *Electr. Pow. Syst. Res.*, vol. 78, no. 4, pp. 559-565, Apr. 2008.
- [20] D. K. Mpoyi, A. L. Ekuakille, M. A. Ugwiri, C. Casavola, and G. Pappaletta, "Wear monitoring based on vibration measurement during machining: an application of FDM and EMD," *Meas. Sens.*, vol. 32, Apr. 2024, Art. no. 101051.
- [21] A. Redekar, H. S. Dhiman, D. Deb, and S. M. Muyeen, "On reliability enhancement of solar PV arrays using hybrid SVR for soiling forecasting based on WT and EMD decomposition methods," *Ain. Shams. Eng. J.*, vol. 15, Jun. 2024, Art. no. 102716.
- [22] Z. Shamaee and M. Mivehchy, "Dominant noise-aided EMD (DEMD): extending empirical mode decomposition for noise reduction by incorporating dominant noise and deep classification," *Biomed. Signal Proces.*, vol. 80, Feb. 2023, Art. no. 104218.
- [23] A. Sadhu, "An integrated multivariate empirical mode decomposition method towards modal identification of structures," *J. Vib. Control.*, vol. 23, no. 17, pp. 2727-2741, Oct. 2017.
- [24] J. M. Liu, X. L. Li, X. Y. Qiao, and H. Y. Li, "Time-frequency analysis of diesel engine cylinder head vibration signal based on EMD and STFT," *Noise. V.*, vol. 33, no. 2, pp. 133-137, Jan. 2013.
- [25] Y. L. Zhu, Y. F. Jia, L. W. Wang, L. Li, and Y. Y. Zheng, "Feature extraction and classification of transformer partial discharge signal based on improved variational mode decomposition and Hilbert transform," *Trans. China. Electrotechnical. Soc.*, vol. 32, no. 9, pp. 221-235, Jan. 2017.
- [26] Z. L. Yang and J. J. Xiong, "Application of parameter-optimized VMD in blasting vibration signal analysis," *J. North. Univ. China. Nat. Sci.*, vol. 41, no. 5, pp. 467-473, Oct. 2020.
- [27] Y. Zheng, X. F. Sun, J. Chen, and J. Yue, "An excellent denoising algorithm for pulse signals while drilling based on ensemble empirical mode decomposition," *Petrol. Explor. Dev.*, vol. 39, no. 6, pp. 750-753, Jan. 2012.
- [28] H. Yang, Y. L. Chen, Y. Xu, and Q. Zhao, "Analysis and study on vibration signals during the startup transient process of hydroelectric generating sets based on the VMD-HHT method," *Adv. Eng. Sci.*, vol. 49, no. 2, pp. 92-99, Jan. 2017.
- [29] C. L. Liu, Y. J. Wu, and C. G. Zhen, "Fault diagnosis of rolling bearings based on variational mode decomposition and fuzzy C-means clustering," *Proc. CSEE.*, vol. 35, no. 13, pp. 3358-3365, Jan. 2015.